



Human Kelch-like protein 20 (KLHL20)



A Target Enabling Package (TEP)

Gene ID / UniProt ID / EC	27252 / Q9Y2M5
Target Nominator	John B. Davis (Alzheimer's Research UK Oxford Drug Discovery Institute, University of Oxford, UK)
SGC Authors	Zhuoyao Chen, Tryfon Zarganes-Tzitzikas, Anindita Sengupta, James M. Bennett, Thomas Christott, Sarah Picaud, Panagis Filippakopoulos, Paul E. Brennan, Oleg Fedorov, Alex N. Bullock
Collaborating Authors	¹ Vincenzo D'Angiolella
Target PI	Alex N. Bullock (SGC Oxford)
Therapeutic Area(s)	Cancer and Neuropsychiatry
Disease Relevance	The E3 ligase KLHL20 is a top 20 biomarker for Alzheimer's disease progression that controls autophagy termination. It also degrades tumour suppressors including PML and DAPK1 to promote cancer.
Date Approved by TEP Evaluation Group	June 10, 2019
Document version	Version 2
Document version date	October 26 th 2020
Citation	Zhuoyao Chen, Tryfon Zarganes-Tzitzikas, Anindita Sengupta, James M. Bennett, Thomas Christott, Sarah Picaud, ... Alex N. Bullock. (2019). Human Kelch-like Protein 20 (KLHL20); A Target Enabling Package [Data set]. Zenodo. 10.5281/zenodo.3245315
Affiliations	¹ Department of Oncology, Cancer Research UK and Medical Research Council Institute for Radiation Oncology, University of Oxford, Oxford OX3 7DQ, UK

USEFUL LINKS



Open Targets



IMPC
International Mouse Phenotyping Consortium

ChEMBL



(Please note that the inclusion of links to external sites should not be taken as an endorsement of that site by the SGC in any way)

SUMMARY OF PROJECT

The BTB-Kelch protein KLHL20 is a hypoxia-induced CUL3-dependent E3 ligase linked to autophagy, Alzheimer's disease and cancer. KLHL20 acts to terminate autophagy by promoting the ubiquitination and degradation of ULK1. KLHL20 is also reported as a top 20 biomarker for Alzheimer's disease progression. Inhibition of KLHL20 may be neuroprotective by extending autophagy for the clearance of neurotoxic proteins aggregates. KLHL20 also promotes cancer through the ubiquitination and degradation of tumour suppressors including PML and DAPK1. We have solved the 1.1 Å structure of the Kelch domain of KLHL20 in complex with a DAPK1 peptide. We have used biophysical and cellular studies to validate this peptide site as a degron site for DAPK1 degradation. Using this peptide, we have also established alpha screen and HTRF assays to identify potent small molecule covalent inhibitors that compete with DAPK1 for binding to the Kelch domain of KLHL20.

SCIENTIFIC BACKGROUND

Kelch-like protein 20 (**KLHL20**, also known as KLEIP) is a member of the BTB-Kelch family that assembles with CUL3 and RBX1 to form a multi-subunit Cullin-RING E3 ligase (1). These complex E3 ligases use the RBX1 subunit to engage a charged E2-ubiquitin pair before transferring the ubiquitin to substrates captured by the BTB-Kelch protein (2,3). Ubiquitination is enhanced by CUL3 neddylation, which stabilizes the correct geometry of the complex for ubiquitin transfer (4).

Like other BTB-Kelch family members, KLHL20 utilises multiple functional domains. The BTB and 3-box domains confer binding to CUL3, whereas the Kelch β -propeller domain serves as the substrate recognition domain. To date, the majority of substrates identified for KLHL20 are targeted for proteasomal degradation, suggesting their modification by Lys48-linked polyubiquitin chains (5). These include the substrates DAPK1 (6), PML (7), PDZ-RhoGEF (8) and ULK1 (9). However, KLHL20 also plays an important role in protein trafficking by targeting coronin 7 to the trans-Golgi network through atypical K33-linked polyubiquitination (10).

The substrates of KLHL20 reflect its function in cellular stress responses as well as its linkage to human disease (5). Transcription of the KLHL20 gene is upregulated by the hypoxia-inducible factor HIF-1 α leading to its overexpression in hypoxic tumour cells (7). In this context KLHL20 can promote tumorigenesis by degrading the tumour suppressor proteins DAPK1 and PML. In human prostate cancer patients higher levels of KLHL20 (and low PML) were found to correlate specifically with high grade tumours (7). Moreover, KLHL20 depletion in PC3 prostate cancer cells restricted the growth of tumour xenografts suggesting KLHL20 as a potential therapeutic target (7). KLHL20 also plays a critical role in autophagy termination by degrading the pool of activated ULK1 (9). Thus, KLHL20 can restrict both apoptotic and autophagic cancer cell death. Importantly interferon stimulation causes the sequestration of KLHL20 in PML-containing nuclear bodies (6). This inhibitory mechanism allows DAPK1 to evade degradation and to accumulate to mediate interferon-induced cell death (6). Notably, the stress responses of KLHL20 also appear linked to neurodegeneration with KLHL20 RNA transcript levels being among the top 20 biomarkers for Alzheimer's disease progression (11,12).

Despite the growing number of substrate proteins identified for the 50 members of the BTB-Kelch family, there remains limited knowledge of their specific binding epitopes and consequently a lack of structural information for the corresponding E3-substrate complexes. Here we have investigated the binding of KLHL20 to DAPK1, which was the first reported substrate for this E3 ligase. Yeast two-hybrid studies previously mapped the interaction to the death domain of DAPK1 and the Kelch domain of KLHL20. Through a peptide scanning approach we identified a 'LPDLV'-containing recruitment site within this DAPK1 region that bound to KLHL20 with low micromolar affinity. We also determined the crystal structure of their complex at 1.1 Å resolution revealing a distinct peptide binding mode compared to the previously determined structural complexes of KEAP1 and KLHL3. The novel structure further identifies a hydrophobic substrate pocket that appears attractive for small molecule inhibitor development. Finally, we have established alpha screen and HTRF assays for compound screening and identified covalent fragments that inhibit DAPK1 binding to KLHL20 with IC₅₀ values in the low micromolar range.

RESULTS – THE TEP

Proteins purified

KLHL20 Kelch domain (used for crystallography and assays)

Human KLHL20 Kelch domain (residues 303-605) was cloned into pNIC28-Bsa4, expressed in BL21(DE3)-R3-pRARE2 cells and purified sequentially using Ni-affinity, size exclusion and anion exchange chromatography.

KLHL3 Kelch domain (used for assays)

Human KLHL3 Kelch domain (residues 298-587) was cloned into pNIC28-Bsa4, expressed in BL21(DE3)-R3-pRARE2 cells and purified sequentially using Ni-affinity, size exclusion and anion exchange chromatography.

Structural data

KLHL20 structures solved at SGC

6GY5 1.09 Å structure of the Kelch domain of KLHL20 in complex with DAPK1 peptide

KLHL20 structures solved elsewhere

5YQ4 1.58 Å structure of the apo-Kelch domain of KLHL20 containing a disulphide bond

Structure and substrate binding of KLHL20 Kelch domain

We have solved the structure of the Kelch domain of KLHL20 in complex with a DAPK1 substrate peptide at 1.09 Å resolution (**Fig. 1**). The structure required the identification of a DAPK1 peptide (LGLPDLVAKYN) suitable for co-crystallisation (see assay section). This peptide contains a central 'LPDLV' motif that was shown to be critical for the interaction with KLHL20. The Kelch domain of KLHL20 shows a canonical β -propeller fold. The six Kelch repeats form the six blades (I-VI) of the propeller arranged radially around a central axis. Each repeat is folded into a twisted β -sheet consisting of four antiparallel β -strands (**Fig. 1**). A final C-terminal β -strand is observed to close the β -propeller and inserts into blade I as the innermost β A strand. Packing between each blade is mediated by a number of conserved hydrophobic positions as well as several buried charged residues that recur within each Kelch repeat. The substrate binding surface on KLHL20 is shaped by the long BC loops which protrude outwards from the Kelch domain surface, and the largely buried DA loops which link adjacent blades and contribute to the protein core.

The bound DAPK1 peptide shows an extended conformation that packs between Kelch domain blades II and III at its N-terminus and blades V and VI at its C-terminus. At its centre the peptide adopts a single loose helical turn that is stabilised by intramolecular hydrogen bonds. Here, the peptide inserts deeply into the central cavity of the Kelch domain β -propeller where it is anchored in the complex by Leu1339, the second leucine in the 'LPDLV' motif. In total, the complex between KLHL20 and DAPK1 includes 8 direct hydrogen bond or salt bridge interactions as well as a number of water-mediated interactions. The critical 'LPDLV' motif of DAPK lies at the core of the protein-peptide interface. Here, the hydrophobic side chains pack against Kelch domain blades I and II and make notable van der Waals contacts with KLHL20 Trp326, His373 and Leu592, respectively. The DAPK1 peptide is derived from the death domain of DAPK1 which has proven intractable for protein work due to its intrinsic disorder and a high propensity for aggregation (13). Modelling indicates that the loose helical turn in the peptide co-structure is likely to match the predicted helix α 3 in the death domain.

To date few Kelch-substrate complexes have been structurally characterized, with the major examples being the KEAP1-NRF2 (14,15) and KLHL3-WNK4 systems (16). The Kelch family proteins are relatively diverse in their primary sequences. Indeed, KLHL20 shares only 25 to 50% sequence identity with other human Kelch domains. Comparison of the available complex structures shows that the substrate binding modes in KEAP1 and KLHL3 are distinct from that of KLHL20. (**Fig. 2**). Notably, the interaction surface in KLHL20 provides a substantial hydrophobic contribution that should make it favourable for inhibitor development.

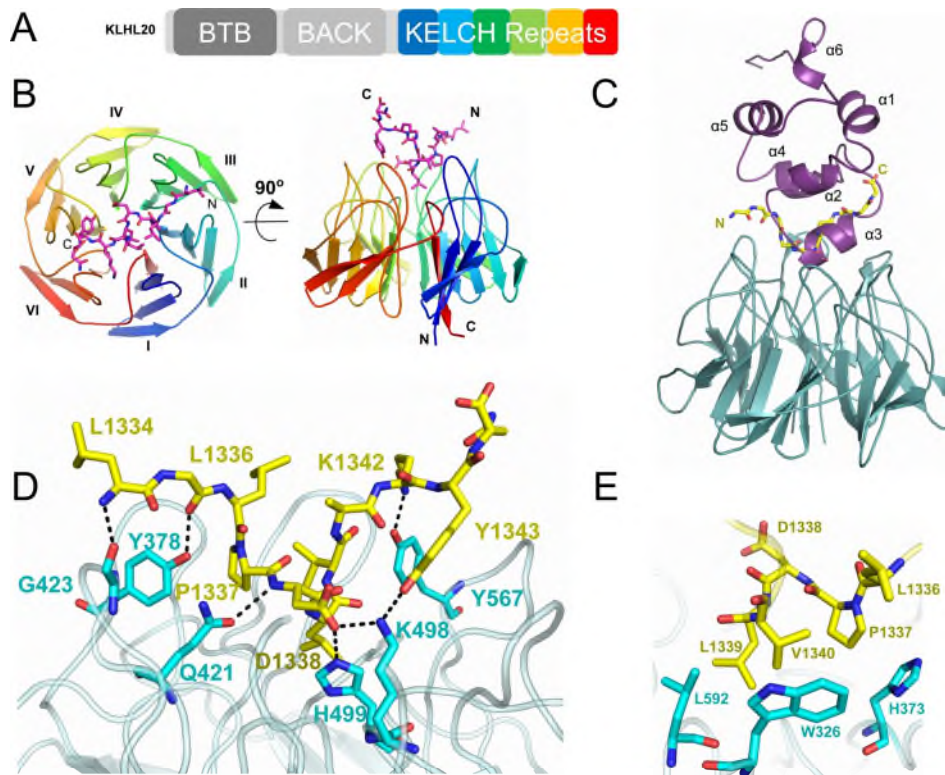


Fig. 1. Structure of KLHL20 Kelch domain bound to DAPK1 peptide. (A) Domain organisation of KLHL20. (B) Overview of the structure showing the Kelch β -propeller and DAPK1 peptide. (C) Superposition of the KLHL20-DAPK1 structure (cyan/yellow) and a homology model of the DAPK1 death domain (purple; template PDB 3MOP) based on the critical 'LPDLV' motifs of DAPK1. (D) Electrostatic interactions in the KLHL20-DAPK1 complex. (E) Key hydrophobic interactions from the DAPK1 'LPDLV' motif.

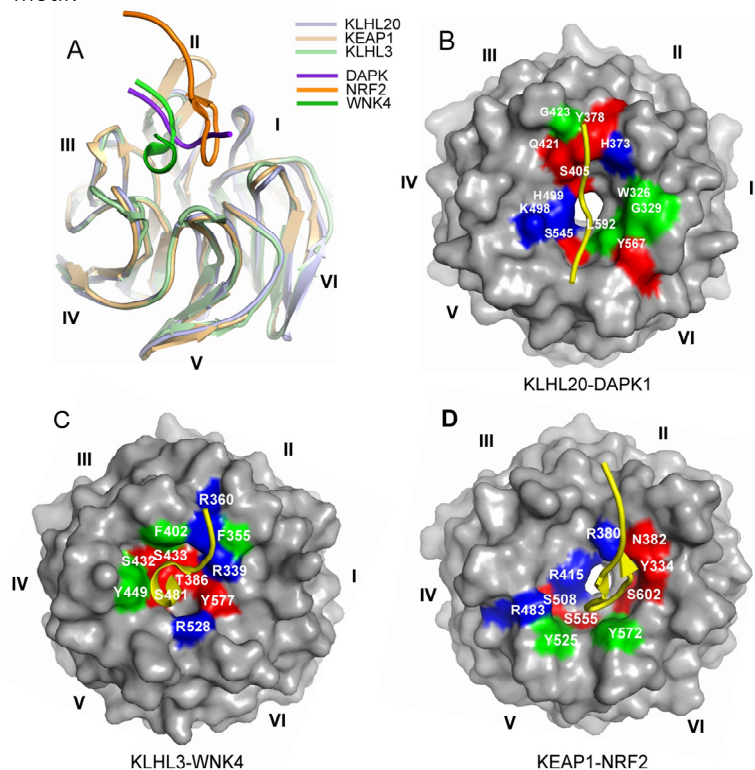


Fig. 2. The binding mode of DAPK1 is distinct from other Kelch-substrate complexes. (A) Superposition of the complex structures of KLHL20-DAPK1 (light and dark purple), KEAP1-NRF2 (PDB 2FLU, light and dark orange) and KLHL3-WNK4 (PDB 4CH9, light and dark green). (B-D) Surface representations of the Kelch domains in the KLHL20-DAPK1 (B), KLHL3-WNK4 (C) and KEAP1-NRF2 (D) complexes with key contact residues highlighted by their binding characteristics (blue, basic residue; red, other polar; green, hydrophobic). The distinct surfaces and bound peptide conformations (yellow ribbons) highlight the rich variety of binding modes that can be established by the circular Kelch domain substrate pockets.

In addition to our structure, an external group in Taiwan has independently solved a structure of KLHL20 in an apo-state (PDB 5YQ4, unpublished). Comparison of the apo and substrate-bound complexes reveals an oxidation in the apo-structure establishing a disulphide bond between two cysteines that are widely separated in our structure. As a result, the disulphide causes significant distortion of the substrate-binding pocket which would likely preclude DAPK1 interaction with this conformation (**Fig.3**).

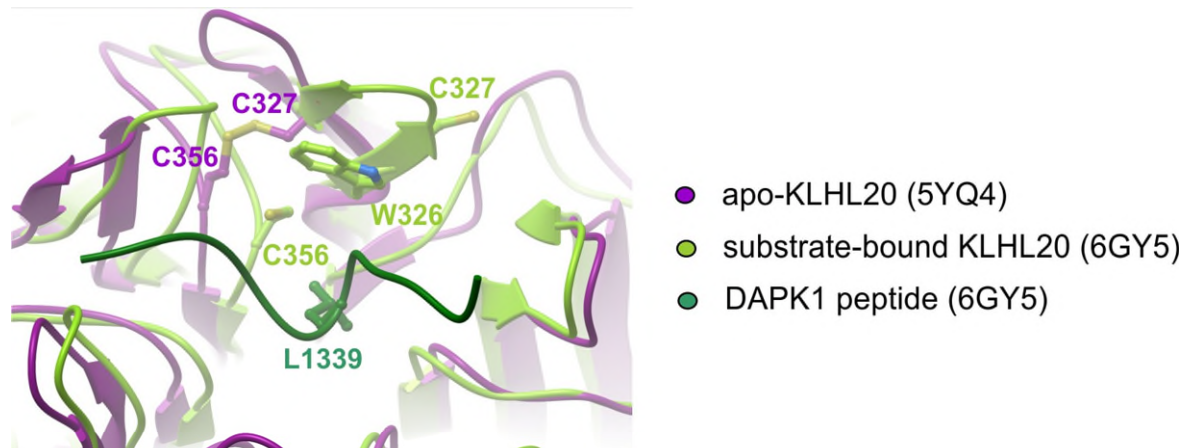


Fig. 3. Comparison of the apo-KLHL20 structure and substrate-bound complex. Superposition of the available structures shows an oxidation in the apo-structure causing a disulphide bond between Cys327 and Cys356. This distorts the substrate binding pocket.

Assays

Mapping of the DAPK1 binding motif for KLHL20 recruitment

Due to the difficulty of making recombinant DAPK1 death domain (**Fig. 4A**) we set out to map the DAPK1 binding epitope using the SPOT peptide technology. We synthesized a peptide array to span the length of the DAPK1 death domain using 15-mer peptides and a three amino acid frameshift at each position. Probing of the array with recombinant 6xHis-KLHL20 Kelch domain and anti-His-antibody for detection revealed protein capture at two sites encompassing DAPK1 residues 1327-1350 and 1378-1395, respectively (**Fig. 4B**). A control experiment indicated that the binding epitope was likely to reside within the N-terminal region since peptides from the second site also bound to the anti-His antibody alone marking them as likely false positives.

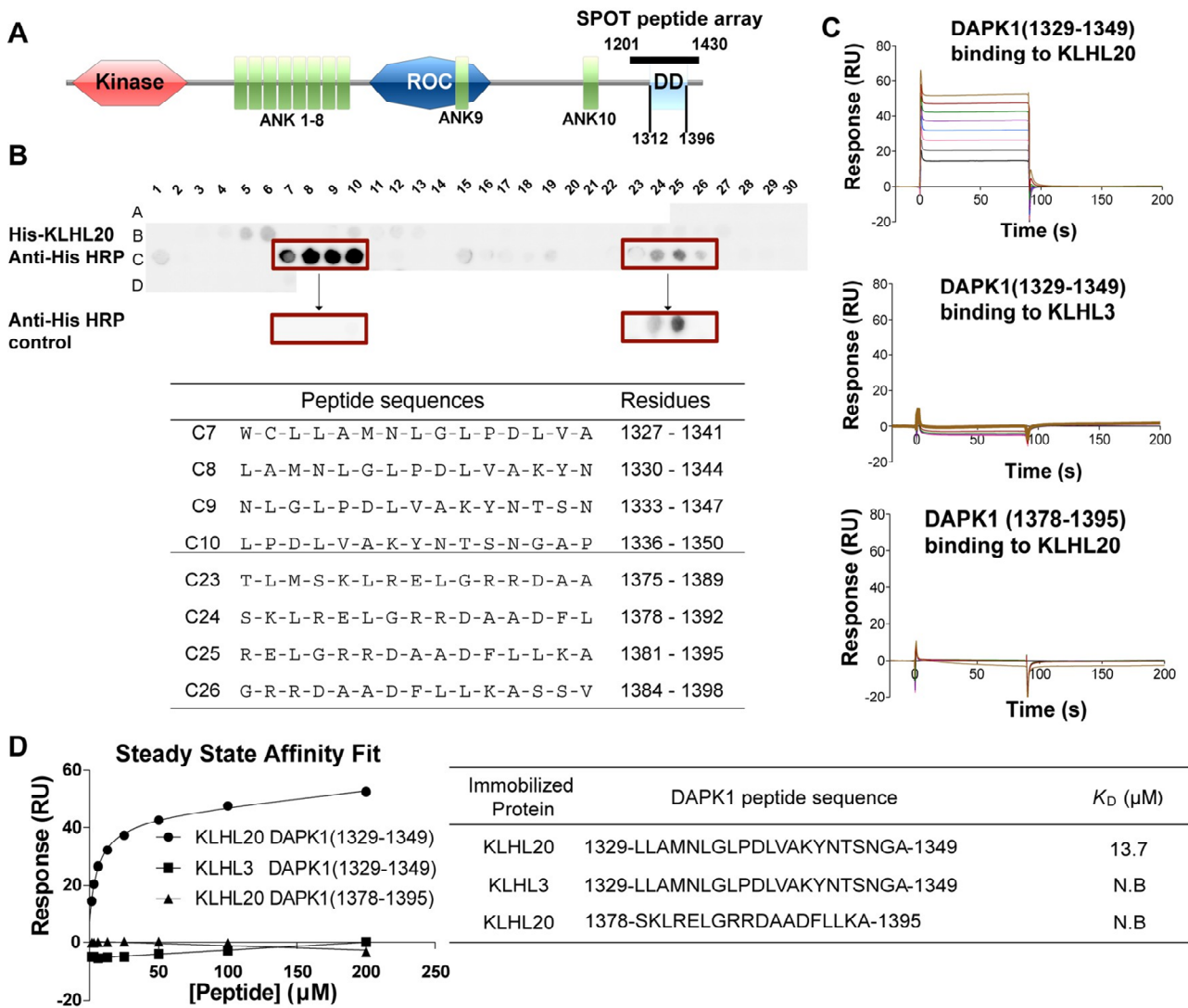


Fig. 4. Mapping of the DAPK1 binding motif for KLHL20 recruitment. **(A)** Domain organization of human DAPK1 (ank, ankyrin repeat; DD, death domain comprising residues 1312 to 1396). The solid horizontal bar denotes the extended region explored for KLHL20 interaction (DAPK1 residues 1201-1430). **(B)** SPOT peptide array. Each spot was printed as a 15-mer DAPK1 peptide with a 3 residue frameshift at each consecutive position. Arrays were incubated with purified 6xHis-KLHL20 Kelch domain, washed and then KLHL20 binding detected using anti-His HRP-conjugated antibody. Binding was observed at two sites spanning DAPK1 residues 1327-1350 and 1378-1395, respectively. As a control, duplicate spots were probed with antibody alone and revealed nonspecific antibody binding to DAPK1 residues 1378-1395. **(C)** For SPR experiments, KLHL20 and KLHL3 Kelch domains were immobilized by amine coupling on different flow cells of a CM5 sensor chip. Indicated DAPK1 peptides were injected subsequently at concentrations of 1.6 μM , 3.1 μM , 6.2 μM , 12.5 μM , 25 μM , 50 μM , 100 μM and 200 μM . Binding was monitored at a flow rate of 30 $\mu\text{L}/\text{min}$. **(D)** SPR binding data were fitted using a steady state affinity equation. DAPK1 residues 1329-1349 bound to KLHL20 Kelch domain with $K_D = 13.7$ μM . (N.B., no binding detected).

To validate these putative interaction sites, we designed peptides for the two DAPK1 regions and performed surface plasmon resonance (SPR) experiments to measure their respective binding affinities for KLHL20 (**Fig. 4C**). A DAPK1 peptide spanning the N-terminal site residues 1329-1349 bound robustly to the Kelch domain of KLHL20 with $K_D = 13.7$ μM (**Fig. 4D**). The same peptide showed no apparent binding to the Kelch domain of KLHL3 demonstrating that the interaction was specific to KLHL20 (**Fig. 4D**). A DAPK1 peptide spanning the C-terminal site residues 1378-1395 also failed to bind to KLHL20 confirming that this downstream region was a false positive (**Fig. 4D**). Together these data identified a single epitope within the death domain of DAPK1 that showed both potency and specificity for interaction with KLHL20.

An 'LPDLV' motif in DAPK1 is critical for KLHL20 interaction

Attempts to crystallise KLHL20 either alone or in complex with the identified 21-mer peptide from DAPK1 produced only microcrystalline material yielding poor diffraction. Therefore, we sought to refine the minimal DAPK1 epitope by using the SPOT technology for peptide truncation experiments as well as alanine scanning to probe the sequence determinants of binding. The results from these experiments were in excellent agreement and identified DAPK1 residues '1336-LPDLV-1340' as critical for KLHL20 interaction (**Fig. 5**).

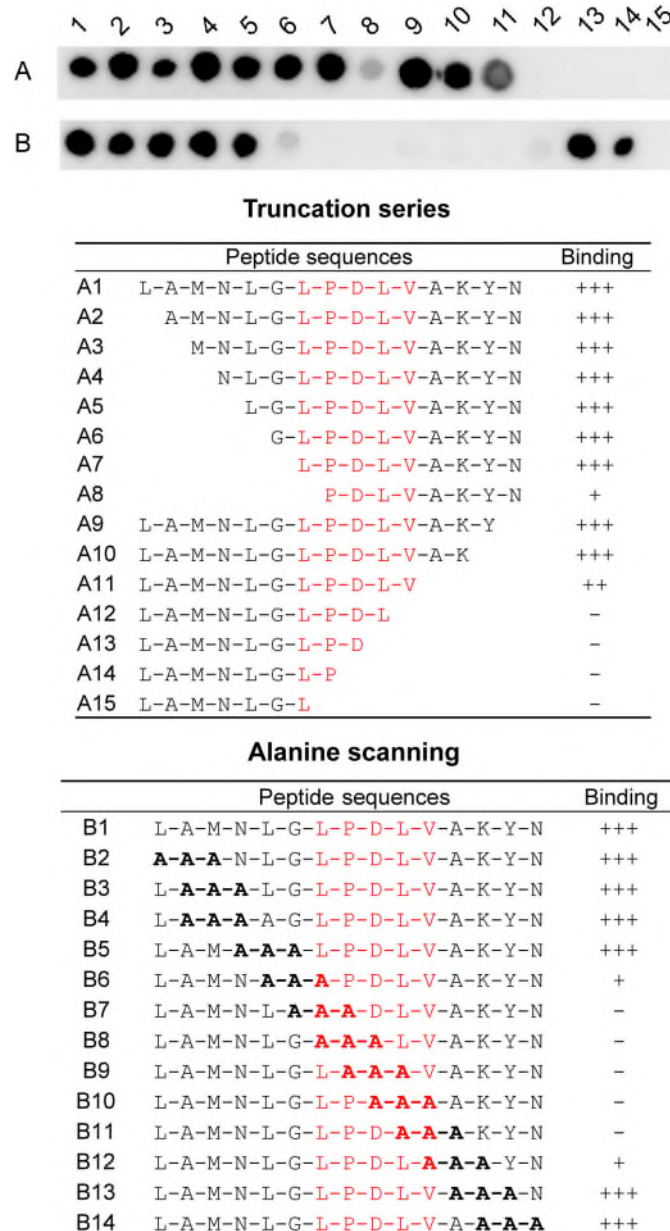


Fig. 5. An 'LPDLV' motif in DAPK1 is critical for KLHL20 interaction. DAPK1 peptide variants were printed in SPOT peptide arrays. Row A peptides explored N and C-terminal truncations whereas row B explored triple-alanine scanning mutagenesis. Arrays were incubated with purified 6xHis-KLHL20 Kelch domain, washed and then binding detected with anti-His antibody. KLHL20 binding was abrogated upon deletion or mutation of a central 'LPDLV' sequence motif in DAPK1.

To validate the identified DAPK1 epitope as a putative degron we generated a full length DAPK1 mutant in which the critical 1336-'LPDLV' motif was mutated to 'LPAAV'. Immunoprecipitation (**Fig. 6A**) of Flag-KLHL20 Kelch domain and HA-DAPK1 full length variants showed that the wild type DAPK1 was bound to KLHL20 whereas the DAPK1 mutant was only recovered at a background level also observed with anti-Flag agarose beads alone. We then performed a cycloheximide (CHX) chase assay to compare the degradation

mechanisms of DAPK1 variants regulated by full length KLHL20. As shown in **Fig. 6B and C**, co-expression of full length KLHL20 protein and DAPK1 WT caused a striking reduction in the half-life of DAPK1 WT compared to expressing DAPK1 WT alone. The DAPK1 mutant appeared strikingly resistant to KLHL20 overexpression consistent with disrupted interaction. The half-life of DAPK1 mutant exceeded that of DAPK1 WT in either condition above. Taken together, these data suggest that the ‘LPDLV’ motif is required for both DAPK1 recruitment and degradation by KLHL20.

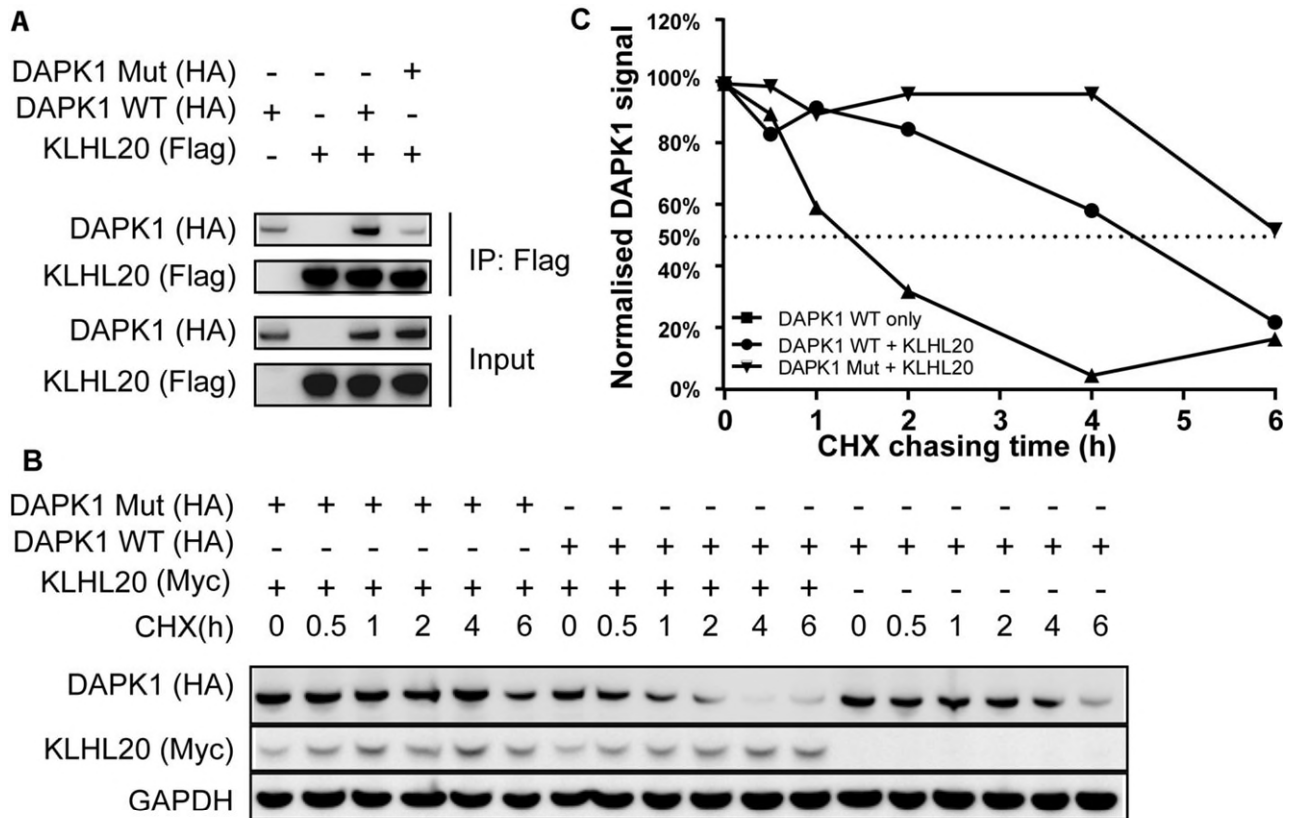


Fig. 6. Mutations in the DAPK1 ‘LPDLV’ motif impair DAPK1 binding and degradation by KLHL20. **(A)** Full length DAPK1 variants and KLHL20 Kelch domain were co-transfected into HEK293T cells as indicated. Flag-KLHL20 Kelch was immunoprecipitated with anti-Flag antibody. DAPK1 WT was robustly co-purified with KLHL20, whereas DAPK1 mutant was only recovered at the background level of the beads alone. **(B)** DAPK1 variants were transfected into HEK293T cells with or without full length KLHL20 as indicated. After 24 hours post transfection, cells were incubated with 100 µg/mL cycloheximide (CHX) and harvested at different time points as indicated. DAPK1 protein levels were detected by Western Blot and normalised to GAPDH. **(C)** Quantitation of **(B)**.

Peptide Displacement Assays

Assays were set up with biotinylated peptide (Biotin-LLAMNLGLPDLVAKYNTSNGA, btn-peptide) and N-terminally hexahistidine tagged protein (6His-protein). For detection, two orthogonal technologies were used; **i.** AlphaScreen technology from Perkin Elmer and **ii.** HTRF from Cisbio. To validate the assays free non-biotinylated peptide was used as a competitor to the 6His-protein:btn-peptide interaction. In the AlphaScreen assay dose response experiments with the non-biotinylated peptide were carried out at three different concentration ratios of 6His-protein to btn-peptide (30 nM/90 nM, 60 nM/60 nM and 120 nM/60 nM). The interaction was interrupted in a dose-dependent manner at single-digit micromolar EC₅₀ values in all three cases (1.1 µM, 1.3 µM and 1.6 µM, respectively) (**Fig. 7**).

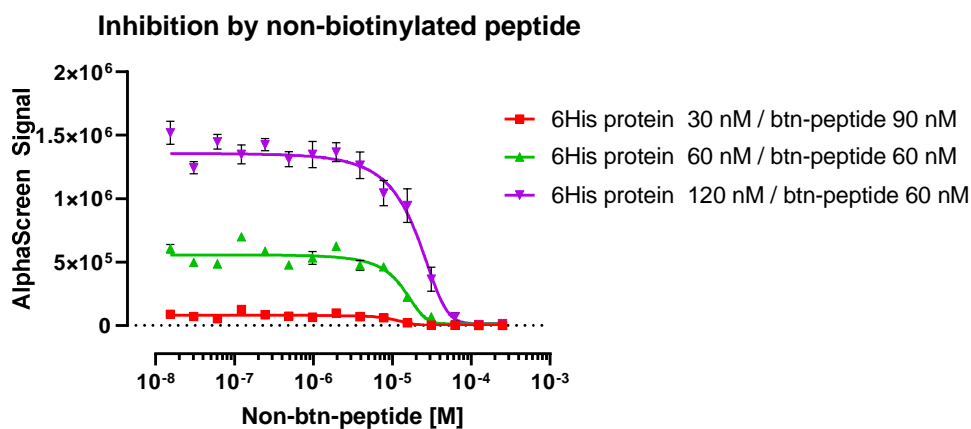


Fig. 7. Dose-dependent inhibition of 6His-protein:btn-peptide interaction in AlphaScreen assay by non-biotinylated peptide. Data points represent mean value of four technical replicates, error bars represent standard deviation.

Further analysis of the substrate-binding pocket in KLHL20 revealed that Cys356 was ideally placed for design of covalent inhibitor development (**Fig. 8**). A collection of some 200 covalent-binding fragments from Nir London (Weizmann) was then screened in the same assays. Compounds were dispensed in duplicate at single concentration (50 μ M) for the initial screen and as 11-point dose response curves starting from 200 μ M for IC₅₀ value determination. Promising hits were observed with IC₅₀ values in the range 0.13 to 15 μ M (see **Table 1** below). Screening was also performed against non-covalent compounds from the 10K MIDAS chemical library. Whilst these data are still in progress the screens indicate that KLHL20 shows promising tractability for non-covalent compounds (**Fig. 9**).

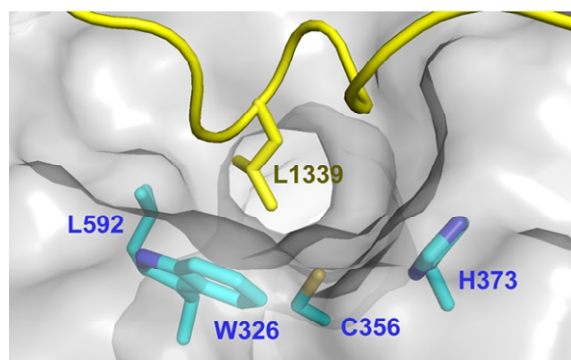


Fig. 8. KLHL20 substrate-binding pocket showing the position of Cys356 is amenable for covalent inhibitor development.

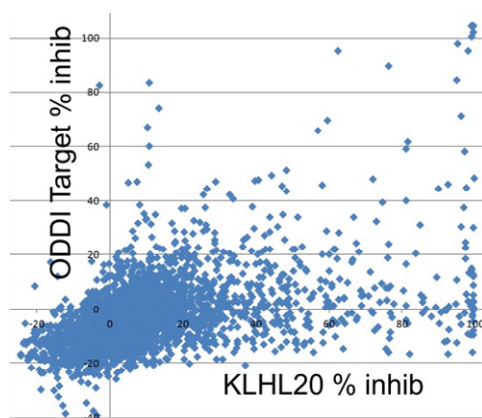
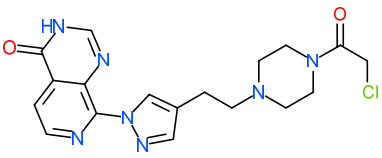
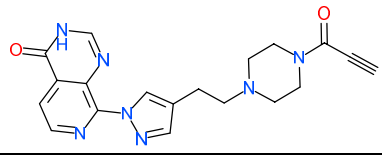
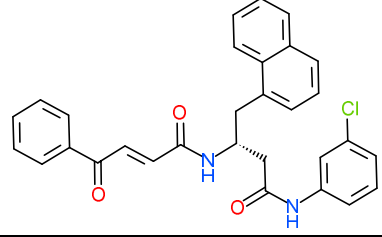
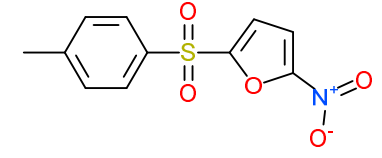
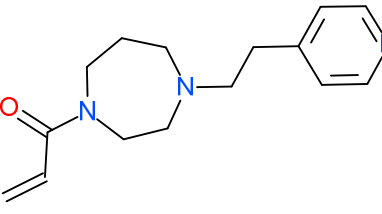
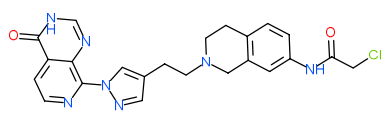
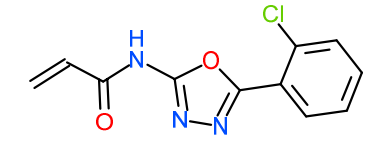
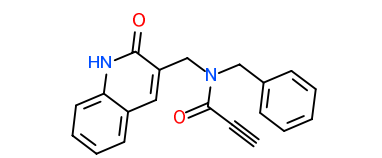
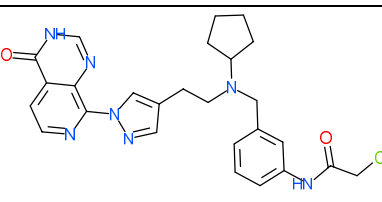
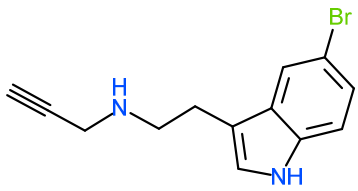
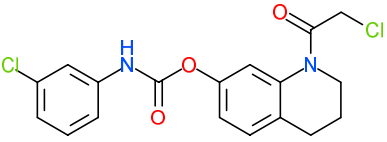
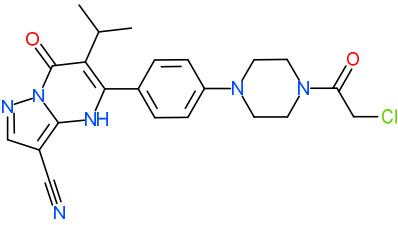
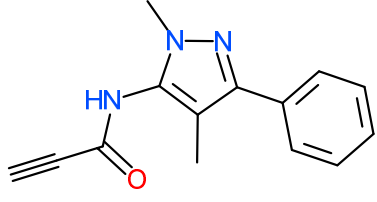
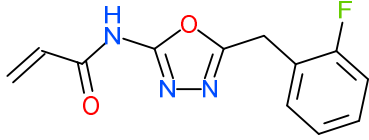


Fig. 9. Single dose (30 μ M) inhibitor screening of the 10K MIDAS library of non-covalent compounds. Hits for KLHL20 are plotted against hits for a counter target screening at the Alzheimer's Research UK Oxford Drug Discovery Institute, University of Oxford, UK.

Chemical Matter – Table 1

Compound ID	Ligand	Chemical Formula	IC ₅₀ μM	Ligand Efficiency	Lipophilic Ligand Efficiency
KD033171		C ₁₈ H ₂₀ ClN ₇ O ₂	0.13	0.34	7.28
KD033835		C ₁₉ H ₁₉ N ₇ O ₂	0.35	0.32	6.29
NU000870		C ₃₀ H ₂₅ ClN ₂ O ₃	0.99	0.23	-0.45
NC001987		C ₁₁ H ₉ N ₂ O ₅ S	1.02	0.47	3.83
DU002253		C ₁₅ H ₂₁ N ₃ O	2.42	0.41	4.17
KD036425		C ₂₃ H ₂₂ ClN ₇ O ₂	4.92	0.23	4.19
DU002364		C ₁₁ H ₈ ClN ₃ O ₂	7.34	0.42	3.04
DU002335		C ₂₀ H ₁₆ N ₂ O ₂	7.44	0.30	0.83
KD036424		C ₂₆ H ₂₈ ClN ₇ O ₂	9.35	0.20	2.08

DU002286		C13H13BrN2	11.08	0.43	1.99
NU000007		C18H16Cl2N2O3	11.96	0.26	1.22
KD002117		C22H23ClN6O2	13.07	0.22	2.77
DU002376		C14H13N3O	14.24	0.38	2.10
DU002319		C12H10FN3O2	15.24	0.38	3.26

IMPORTANT: Please note that the existence of small molecules within this TEP indicates only that chemical matter might bind to the protein in potentially functionally relevant locations. The small molecule ligands are intended to be used as the basis for future chemistry optimisation to increase potency and selectivity and yield a chemical probe or lead series. As such, the molecules within this TEP should not be used as tools for functional studies of the protein, unless otherwise stated, as they are not sufficiently potent or well-characterised to be used in cellular studies.

Antibodies

Commercial antibodies against KLHL20 are available, although they have not been validated at the SGC.

CRISPR/Cas9 reagents

CRISPR/Cas9 reagents for KLHL20 are described in commercial catalogues, although they have not been tested at the SGC.

Future plans

Co-crystallisation of the covalent screening compounds is in progress to determine their binding mode. Further screening against libraries of non-covalent compounds is also underway. Chemistry is planned to develop these hits into chemical probes.

Collaborations

Vincenzo D'Angiolella (Oxford, Oncology Dept) – cellular assays.

CONCLUSION

The BTB-Kelch family E3 ligase KLHL20 has emerged as a high interest protein for inhibitor development due to its links to both Alzheimer's disease and cancer. We speculate that KLHL20 inhibition may help to enhance autophagy-mediated clearance of neurotoxic aggregates consistent with its linkage to Alzheimer's disease progression. In cancer it may additionally help to stabilise tumour suppressor proteins including PML and

DAPK1. PML expression, in particular, is lost in a wide range of human cancer in addition to the PML-RAR α fusion found in acute promyelocytic leukaemia (17). Here we have mapped the first degron motif for binding to KLHL20 and solved the first crystal structure of a KLHL20-DAPK1 complex. The identification of a binding peptide enabled the crystallography but also enabled the development of AlphaScreen and HTRF assays for compound screening. This work has led to identification of covalent fragments with low micromolar inhibitory activity against KLHL20 and is work is ongoing for non-covalent inhibitors. Overall the substrate-binding pocket in KLHL20 appears to be attractive for inhibitor development with tryptophan and other hydrophobic residues in the Kelch domain site. Chemical binders at this pocket may also be used in future as “E3 handles” for PROTAC development.

TEP IMPACT

Further collaborations

New collaborations are being formed with pharma to develop a chemical probe against KLHL20. A key aim in this respect is to establish the selectivity of the chemical matter. A collaboration is also newly established with John Davis (Alzheimer's Research UK Oxford Drug Discovery Institute, University of Oxford, UK) to explore the potential of KLHL20 as a target for autophagy regulation in Alzheimer's disease.

Publications arising from this work:

- Chen, Z., Picaud, S., Filippakopoulos, P., D'Angiolella, V., Bullock, A.N. [Structural basis for recruitment of DAPK1 to the KLHL20 E3 ligase.](#) (2018) bioRxiv

FUNDING INFORMATION

The work performed at the SGC has been funded by a grant from Wellcome [106169/ZZ14/Z]. Zhuoyao Chen acknowledges DPhil support from a China Scholarship Council-University of Oxford Scholarship.

ADDITIONAL INFORMATION

Structure Files

PDB ID	Structure Details
6GY5	1.09 Å structure of KLHL20 Kelch domain with DAPK1 peptide

Materials and Methods

Mass Spectrometry

Protein masses were determined using an Agilent LC/MSD TOF system with reversed-phase high-performance liquid chromatography coupled to electrospray ionisation and an orthogonal time-of-flight mass analyser. Proteins were desalted prior to mass spectrometry by rapid elution off a C3 column with a gradient of 5-95% isopropanol in water with 0.1% formic acid. Spectra were analysed using the MassHunter software (Agilent).

Protein Expression and Purification

Human KLHL20 Kelch domain

Boundaries: residues 303-605

Expressed protein sequence:

MHHHHHHSSGVDLGTENLYFQSMQGPRTPRKPIRCGEVLFAVGGWCSGDAISSVERYDPQTNEWRMVASMSKRRCG
VGVSVLDDLLYAVGGHDGSSYLNSVERYDPKTNQWSSDVAPTSTCRTSVGVAVLGGFLYAVGGQDGVSLNIVERYDPKE
NKWTRVASMSTRRLGVAVAVLGGFLYAVGGSDGTSPLNTVERYNPQENRWHTIAPMGTRRKHLGCAVYQDMIYAVGGR
DDTTELSAERYNPRTNQWSPVAMTSRRSGVGLAVVNGQLMAVGGFDGTTYLKTIEVFPDANTWRLYGGMNYRRLG
GGVGVKIMTHCE

Vector: pNIC28-Bsa4

Tag and additions: TEV-cleavable N-terminal hexahistidine tag

Expression cell: E. coli BL21(DE3)R3-pRARE2

The Kelch domain of human KLHL20 (Uniprot Q9Y2M5 isoform 1, M303-E605) was cloned using ligation-independent cloning into the bacterial expression vector pNIC28-Bsa4 (GenBank accession number EF198106) which provides for an N-terminal hexahistidine tag and TEV cleavage site. Plasmid DNA was transformed into *E. coli* strain BL21(DE3)R3-pRARE2. Cells were cultured in LB broth at 37°C until OD₆₀₀ reached 0.6. Recombinant protein expression was then induced by addition of 0.4 mM isopropyl β-D-1-thiogalactopyranoside followed by 18 hours continuous shaking at 18°C. Cells were harvested by centrifugation and lysed by sonication in binding buffer (50 mM HEPES pH 7.5, 500 mM NaCl, 5% glycerol, 5 mM imidazole) supplemented with 0.5 mM TCEP. Recombinant proteins were captured on nickel sepharose resin, washed with binding buffer and eluted by a stepwise gradient of 30-250 mM imidazole. Further clean-up was performed by size exclusion chromatography using a HiLoad 16/600 S200 Superdex column buffered in 50 mM HEPES pH 7.5, 300 mM NaCl, 0.5 mM TCEP. Finally, the eluted protein was purified by anion exchange chromatography using a 5 mL HiTrap Q column. Protein masses were confirmed by intact LC-MS mass spectrometry. Where required, the hexahistidine tag was cleaved overnight at 4°C using TEV protease.

Human KLHL3 Kelch domain

Boundaries: residues 298-587

Expressed protein sequence:

MHHHHHHSSGVDLGTENLYFQSMPLPKVMIVVGGQAPKAIRSVECYDFEEDRWQIAELPSRRRCRAGVVFVFMAGHVYAV
GGFNGSLRVRTVDVYDGVKQWTSIASMQERRSTLGA AVLNDLLYAVGGFDGSTGLASVEAYS YKTNEWFFVAPMNTTR
SSVGVGVVEGKLYAVGGYD GASRQCLSTVEQYNPATNEWIYVADMSTRRSGAGVGVLSGQLYATGGHDG PLVRKSVEVY
DPGTNTWKQVADMNMCRRNAGVCAVNGLLYVVGDDGSCNLASVEYYNPVTDKWTLLPTNMSTGRSYAGVAVIHKS L

Vector: pNIC28-Bsa4

Tag and additions: TEV-cleavable N-terminal hexahistidine tag

Expression cell: E. coli BL21(DE3)R3-pRARE2

The Kelch domain of human KLHL3 (Uniprot Q9UH77 isoform 1, residues S298–L587) was cloned into the bacterial expression vector pNIC28-Bsa4. Plasmid DNA was transformed into *E. coli* strain BL21(DE3)R3-pRARE2. Cells were cultured in LB broth at 37°C until OD₆₀₀ reached 0.6. Recombinant protein expression was then induced by addition of 0.4 mM isopropyl β-D-1-thiogalactopyranoside, followed by 18 hours continuous shaking at 18°C. Cells were harvested by centrifugation and lysed by sonication in binding buffer (50 mM HEPES pH 7.5, 500 mM NaCl, 5% glycerol, 5 mM imidazole) supplemented with 0.5 mM TCEP. Recombinant proteins were captured on nickel sepharose resin, washed with binding buffer and eluted by a stepwise gradient of 30-250 mM imidazole. Further clean-up was performed by size exclusion chromatography using a HiLoad 16/600 S200 Superdex column buffered in 50 mM HEPES pH 7.5, 300 mM NaCl, 0.5 mM TCEP. Finally, the eluted protein was purified by anion exchange chromatography using a 5 mL HiTrap Q column. Protein masses were confirmed by intact LC-MS mass spectrometry. Where required, the hexahistidine tag was cleaved overnight at 4°C using TEV protease.

Structures

Structure of the KLHL20-DAPK1 complex

The purified KLHL20 Kelch domain was concentrated to 12 mg/mL using a 10 kDa molecular-mass cut-off centrifugal concentrator in 50 mM HEPES pH 7.5, 300 mM NaCl and 5 mM TCEP buffer. The 11-residue DAPK1 peptide (LGLPDLVAKYN) was purchased from LifeTein and added in the same buffer to a final concentration of 3 mM. The protein-peptide mixture was incubated on ice for 1 hour prior to setting up sitting-drop vapour-diffusion crystallisation plates. Micro-seed stocks were prepared from small KLHL20 crystals grown during previous rounds of crystal optimisation. Those early crystals were transferred into an Eppendorf tube containing 50 μL reservoir solution and a seed bead (Hampton Research), then vortexed for 2 min. Seed stocks were diluted 500-fold before use. The best-diffracting crystals of the KLHL20 complex were obtained at 20°C by mixing 75 nL protein, 20 nL diluted seed stock and 75 nL of a reservoir solution containing 2 M sodium chloride and 0.1 M acetate buffer pH 4.5. Prior to vitrification in liquid nitrogen, crystals were cryoprotected by direct addition of reservoir solution supplemented with 25 % ethylene glycol. Diffraction data were collected on beamline I03 at Diamond Light Source, Didcot, UK. Data were processed in PHENIX version 1.9 (18). Molecular replacement was performed with PHENIX Phaser-MR using KLHL12 (PDB 2VPJ chain A) as the search model. PHENIX Autobuild was used to build the initial structural model. COOT (19) was used for manual model building and refinement whereas PHENIX REFINER was used for automated refinement. TLS parameters were included at later stages of refinement. Tools in COOT, PHENIX and MolProbity (20) were used to validate the structure.

Homology model

A homology model for the death domain of human DAPK1 was built in Molsoft ICM-Pro software using MyD88 (PDB 3MOP chain A, 25% sequence identity) as the structural template. The initial model was refined by energy minimisation and side chain optimisation in ICM-Pro (Molsoft) (21).

Assays

Peptide arrays (SPOT assay)

Cellulose-bound peptide arrays were prepared employing standard Fmoc solid phase peptide synthesis using a MultiPep-RSi-Spotter (INTAVIS, Köln, Germany) as previously described (22). After array synthesis, membranes were incubated with 5% BSA to block free sites. The arrays were then incubated with 1 μM recombinant hexahistidine-tagged KLHL20 Kelch domain in PBS at 4°C overnight. Unbound protein was washed off in PBS buffer with 0.1% Tween 20 and bound protein was detected using HRP-conjugate anti-His antibody Merck Millipore (Cat #71840).

Surface Plasmon Resonance

Assays were performed at 25°C using a BIACORE S200 (GE Healthcare) surface plasmon resonance (SPR) instrument. The Kelch domains of KLHL20 and KLHL3 were immobilised on sensor chip CM5 (GE Healthcare) using amine coupling. Reference flow cells had no immobilised protein. Binding was monitored using a flow rate of 30 μL/min. The peptide analytes were prepared in HBS-P buffer (GE Healthcare). Data reported were after reference flow cell signal subtraction. Data were analysed by one-site steady-state affinity analysis using

the Biacore S200 Evaluation software and the fitting equation $R_{eq} = \frac{CR_{max}}{K_D + C} + RI$ (RI , bulk refractive index contribution; K_D , dissociation constant; C , analyte concentration; R_{max} , maximum response). Peptides were purchased from Severn Biotech.

Co-immunoprecipitation of KLHL20 and DAPK1

HEK293T cells were cultured in high glucose Dulbecco's Modified Eagle's Medium (Sigma-Aldrich) with 5% Penicillin Streptomycin (ThermoFisher) and 10% Fetal Bovine Serum (Sigma-Aldrich) inside a 5% CO₂ incubator at 37°C. KLHL20 Kelch domain (residues M303-T602) and full length DAPK1 constructs were transfected into HEK293T cells at 60% confluency with polyethylenimine. 40 hours after transfection, cells were harvested and lysed in the presence of protease and phosphatase inhibitors. Flag immunoprecipitation was performed using ANTI-FLAG® M2 Affinity Gel (Sigma-Aldrich). Results were analysed using Western blotting (Flag antibody – Sigma-Aldrich, F1804; HA antibody – Biolegend, 901501; Myc antibody – Cell signalling, 2040S). Full length DAPK1 was cloned into pcDNA3.1(+). KLHL20 Kelch domain was cloned into pcDNA3-N-Flag-LIC.

Cycloheximide chase assay

HEK293T cells were cultured as described above until 60% confluency. Full length KLHL20 and DAPK1 constructs were transfected with polyethylenimine. 24 hours after transfection, 100 µg/mL cycloheximide was added to inhibit protein synthesis. Cells were harvested at different time points – 0, 0.5h, 1h, 2h, 4h and 6h. Results were analysed using Western blotting with corresponding antibodies. GAPDH level in each sample was also detected for control (anti-GAPDH antibody; Thermo Fisher, MA5-15738). Western blot band intensities were quantified using Image Studio Lite Ver 5.2 and normalised for the GAPDH control. Full length KLHL20 was cloned into pRK5 (myc tag).

Peptide Displacement Assays

Assays were set up with biotinylated peptide (Biotin-LLAMNLGLPDLVAKYNTSNGA, btn-peptide) and N-terminally hexahistidine tagged protein (6His-protein). For detection, two orthogonal technologies were used; **i.** AlphaScreen technology from Perkin Elmer and **ii.** HTRF from Cisbio. To determine optimal assay conditions for each protein prep, 6His-protein and btn-peptide were titrated against each other in a 16 by 16 matrix in 1:1 dilutions, starting from 800 nM. For the final ratio of 6His-protein and btn-peptide to use in the assay, the point representing the EC₉₀ in the two-dimensional titration was chosen. Typically, final assay concentrations for 6His-protein and btn-peptide fell between 20 and 200 nM. For the AlphaScreen assay, AlphaScreen Histidine (Nickel Chelate) Detection Kit donor and acceptor beads were used at a 1:2500 dilution from purchased stock; for HTRF, SA-XL665 and anti-6His antibody were used at 50 nM and 0.125 nM, respectively. Assays were performed on 384-well ProxiPlates (Perkin Elmer) at a final volume of 20 µL and plates were read using a Pherastar FSX plate reader (BMG Labtech). For inhibitor screening, compounds were dispensed in duplicate at single concentration (typically 30-50 µM) for the initial screen and as 11-point dose response curves starting from 200 µM for IC₅₀ value determination.

References

1. Hara, T., Ishida, H., Raziuddin, R., Dorkhom, S., Kamijo, K., and Miki, T. (2004) [Novel kelch-like protein, KLEIP, is involved in actin assembly at cell-cell contact sites of Madin-Darby canine kidney cells.](#) *Mol Biol Cell* **15**, 1172-1184
2. Genschik, P., Sumara, I., and Lechner, E. (2013) [The emerging family of CULLIN3-RING ubiquitin ligases \(CRL3s\): cellular functions and disease implications.](#) *EMBO J* **32**, 2307-2320
3. Petroski, M. D., and Deshaies, R. J. (2005) [Function and regulation of cullin-RING ubiquitin ligases.](#) *Nat Rev Mol Cell Biol* **6**, 9-20
4. Duda, D. M., Borg, L. A., Scott, D. C., Hunt, H. W., Hammel, M., and Schulman, B. A. (2008) [Structural insights into NEDD8 activation of cullin-RING ligases: conformational control of conjugation.](#) *Cell* **134**, 995-1006
5. Chen, H. Y., Liu, C. C., and Chen, R. H. (2016) [Cul3-KLHL20 ubiquitin ligase: physiological functions, stress responses, and disease implications.](#) *Cell Div* **11**, 5

6. Lee, Y. R., Yuan, W. C., Ho, H. C., Chen, C. H., Shih, H. M., and Chen, R. H. (2010) [The Cullin 3 substrate adaptor KLHL20 mediates DAPK ubiquitination to control interferon responses.](#) *EMBO J* **29**, 1748-1761
7. Yuan, W. C., Lee, Y. R., Huang, S. F., Lin, Y. M., Chen, T. Y., Chung, H. C., Tsai, C. H., Chen, H. Y., Chiang, C. T., Lai, C. K., Lu, L. T., Chen, C. H., Gu, D. L., Pu, Y. S., Jou, Y. S., Lu, K. P., Hsiao, P. W., Shih, H. M., and Chen, R. H. (2011) [A Cullin3-KLHL20 Ubiquitin Ligase-Dependent Pathway Targets PML to Potentiate HIF-1 Signaling and Prostate Cancer Progression.](#) *Cancer Cell* **20**, 214-228
8. Lin, M. Y., Lin, Y. M., Kao, T. C., Chuang, H. H., and Chen, R. H. (2011) [PDZ-RhoGEF ubiquitination by Cullin3-KLHL20 controls neurotrophin-induced neurite outgrowth.](#) *J Cell Biol* **193**, 985-994
9. Liu, C. C., Lin, Y. C., Chen, Y. H., Chen, C. M., Pang, L. Y., Chen, H. A., Wu, P. R., Lin, M. Y., Jiang, S. T., Tsai, T. F., and Chen, R. H. (2016) [Cul3-KLHL20 Ubiquitin Ligase Governs the Turnover of ULK1 and VPS34 Complexes to Control Autophagy Termination.](#) *Mol Cell* **61**, 84-97
10. Yuan, W. C., Lee, Y. R., Lin, S. Y., Chang, L. Y., Tan, Y. P., Hung, C. C., Kuo, J. C., Liu, C. H., Lin, M. Y., Xu, M., Chen, Z. J., and Chen, R. H. (2014) [K33-Linked Polyubiquitination of Coronin 7 by Cul3-KLHL20 Ubiquitin E3 Ligase Regulates Protein Trafficking.](#) *Mol Cell* **54**, 586-600
11. Arefin, A. S., Mathieson, L., Johnstone, D., Berretta, R., and Moscato, P. (2012) [Unveiling clusters of RNA transcript pairs associated with markers of Alzheimer's disease progression.](#) *PLoS One* **7**, e45535
12. Gomez Ravetti, M., Rosso, O. A., Berretta, R., and Moscato, P. (2010) [Uncovering molecular biomarkers that correlate cognitive decline with the changes of hippocampus' gene expression profiles in Alzheimer's disease.](#) *PLoS One* **5**, e10153
13. Dioletis, E., Dingley, A. J., and Driscoll, P. C. (2013) [Structural and functional characterization of the recombinant death domain from death-associated protein kinase.](#) *PLoS One* **8**, e70095
14. Fukutomi, T., Takagi, K., Mizushima, T., Ohuchi, N., and Yamamoto, M. (2014) [Kinetic, thermodynamic, and structural characterizations of the association between Nrf2-DLGex degron and Keap1.](#) *Mol Cell Biol* **34**, 832-846
15. Lo, S. C., Li, X., Henzl, M. T., Beamer, L. J., and Hannink, M. (2006) [Structure of the Keap1:Nrf2 interface provides mechanistic insight into Nrf2 signaling.](#) *EMBO J* **25**, 3605-3617
16. Schumacher, F. R., Sorrell, F. J., Alessi, D. R., Bullock, A. N., and Kurz, T. (2014) [Structural and biochemical characterization of the KLHL3-WNK kinase interaction important in blood pressure regulation.](#) *Biochem J* **460**, 237-246
17. Salomoni, P., Dvorkina, M., and Michod, D. (2012) [Role of the promyelocytic leukaemia protein in cell death regulation.](#) *Cell Death Dis* **3**, e247
18. Adams, P. D., Afonine, P. V., Bunkoczi, G., Chen, V. B., Davis, I. W., Echols, N., Headd, J. J., Hung, L. W., Kapral, G. J., Grosse-Kunstleve, R. W., McCoy, A. J., Moriarty, N. W., Oeffner, R., Read, R. J., Richardson, D. C., Richardson, J. S., Terwilliger, T. C., and Zwart, P. H. (2010) [PHENIX: a comprehensive Python-based system for macromolecular structure solution.](#) *Acta Crystallogr D Biol Crystallogr* **66**, 213-221
19. Emsley, P., and Cowtan, K. (2004) [Coot: model-building tools for molecular graphics.](#) *Acta Crystallogr D Biol Crystallogr* **60**, 2126-2132
20. Chen, V. B., Arendall, W. B., 3rd, Headd, J. J., Keedy, D. A., Immormino, R. M., Kapral, G. J., Murray, L. W., Richardson, J. S., and Richardson, D. C. (2010) [MolProbity: all-atom structure validation for macromolecular crystallography.](#) *Acta Crystallogr D Biol Crystallogr* **66**, 12-21
21. Abagyan, R., Batalov, S., Cardozo, T., Totrov, M., Webber, J., and Zhou, Y. (1997) [Homology modeling with internal coordinate mechanics: deformation zone mapping and improvements of models via conformational search.](#) *Proteins Suppl* **1**, 29-37
22. Picaud, S., and Filippakopoulos, P. (2015) [SPOTting Acetyl-Lysine Dependent Interactions.](#) *Microarrays (Basel)* **4**, 370-388

We respectfully request that this document is cited using the DOI value as given above if the content is used in your work.